



OPEN

Desmosine-Inspired Cross-Linkers for Hyaluronan Hydrogels

SUBJECT AREAS:

BIOINSPIRED MATERIALS
BIOPOLYMERS
TISSUE ENGINEERING
BIOMEDICAL ENGINEERINGValentin Hagel^{1,6*}, Markus Mateescu^{2*}, Alexander Southan^{3*}, Seraphine V. Wegner^{1,6}, Isabell Nuss^{1,6}, Tamás Haraszti^{1,6}, Claudia Kleinhans³, Christian Schuh⁴, Joachim P. Spatz^{1,6}, Petra J. Kluger⁴, Monika Bach^{3,4}, Stefan Tussetschläger², Günter E. M. Tovar^{3,4}, Sabine Laschat² & Heike Boehm^{1,5,6}

¹Department of New Materials and Biosystems, Max Planck Institute for Intelligent Systems Heisenbergstr. 3, 70569 Stuttgart (Germany), ²Institut für Organische Chemie, Universität Stuttgart, Pfaffenwaldring 55, 70569 Stuttgart (Germany), ³Institut für Grenzflächenverfahrenstechnik und Plasmatechnologie IGVP, Nobelstr. 12, 70569 Stuttgart (Germany), ⁴Fraunhofer Institut für Grenzflächen- und Bioverfahrenstechnik IGB Nobelstr. 12, 70569 Stuttgart (Germany), ⁵CSF Biomaterials & Cellular Biophysics, Max Planck Institute for Intelligent Systems Heisenbergstr. 3, 70569 Stuttgart (Germany), ⁶Department of Biophysical Chemistry, University of Heidelberg (Germany).

Received
15 March 2013Accepted
31 May 2013Published
20 June 2013

Correspondence and requests for materials should be addressed to H.B. (heike.boehm@is.mpg.de); S.L. (sabine.laschat@oc.uni-stuttgart.de) or G.E.M.T. (Guentertovar@igvt.uni-stuttgart.de)

* These authors contributed equally to this work.

We designed bioinspired cross-linkers based on desmosine, the cross-linker in natural elastin, to prepare hydrogels with thiolated hyaluronic acid. These short, rigid cross-linkers are based on pyridinium salts (as in desmosine) and can connect two polymer backbones. Generally, the obtained semi-synthetic hydrogels are form-stable, can withstand repeated stress, have a large linear-elastic range, and show strain stiffening behavior typical for biopolymer networks. In addition, it is possible to introduce a positive charge to the core of the cross-linker without affecting the gelation efficiency, or consequently the network connectivity. However, the mechanical properties strongly depend on the charge of the cross-linker. The properties of the presented hydrogels can thus be tuned in a range important for engineering of soft tissues by controlling the cross-linking density and the charge of the cross-linker.

The future challenges of an aging society and the corresponding increase in the need for regenerative medical devices have stimulated worldwide research efforts in the field of tissue engineering. Particular attention has been focused on hydrogels^{1–7} including those made from polymers such as polyethylene glycol diacrylates (PEG-DA)⁸, polyglycerol diacrylates^{9,10}, and chemically modified hyaluronic acid (HA)¹¹, exploiting their hydrophilicity as well as high biocompatibility.

Hyaluronic acid is an evolutionary well-preserved, linear, polyanionic sugar¹² found in all connective tissues¹³ that can promote elastin formation in tissue culture¹⁴. HA-based hydrogels have been studied extensively and thiolated HA (HA-SH) has been shown to be especially well-suited for cell culture applications¹⁵. HA-SH cross-linked with relatively long PEG-DA or gelatin-DA is also commercially available from GlycosanTM¹⁶. Elasticity measurements of these hybrid HA-SH hydrogels cross-linked with PEG-DA showed compression moduli up to 280 kPa¹⁷.

With neutral cross-linkers, HA-SH forms polyanionic hydrogels. Together with the chemical nature, the charge density has been reported to play a role in cell attachment¹⁸, viability¹⁹ and proliferation^{20,21}. However, little is known about how the charge density itself would affect cell behavior, independent of the cross-linker density and chemistry.

Here we compare short, rigid cross-linkers, similar to those found in natural elastic tissue: a neutral one and one carrying a positive charge, but the same reactive groups. In particular, we were interested in desmosine (Figure 1), which is the cross-linker in natural elastin. In the human body, elastin provides the elastic properties of connective tissues. Its elastic protein fibers interact with their hydrophobic amino acids and their lysine side groups are covalently coupled by lysyl oxidase to form desmosine²². Inspired by this structure, as well as recent results from Aida with dendritic oligo-cation cross-linkers²³, we designed new rigid cross-linkers based on pyridinium salts tethered by short spacers to acrylate or acrylamide units that can react with HA-SH by the thiol-Michael addition. From the desmosine structure we included the aromatic core ring with the pyridinium salt^{24–29}, containing a positive charge, and two of the short arms with reactive groups at the ends (Figure 2). Pyridinium derivatives were chosen because the chemistry is well established, a positive charge can be easily introduced by N-alkylation³⁰, and they should display sufficient water solubility for gel formation. In natural elastin, four lysine side chains build up one desmosine and connect two backbones via two arms on each side²².

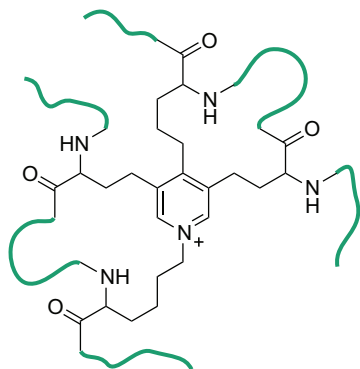


Figure 1 | Desmosine in its linked state connects two elastin backbones.

We used two-armed cross-linkers rather than four-armed cross-linkers to prevent the linker from connecting to more than two backbones.

Results

We synthesized six artificial cross-linkers with this geometry, which are shown in **Figure 2**. We were particularly interested in which of these cross-linkers would yield stable, biocompatible hydrogels with the polyanionic HA-SH and how the additional charge on the nitrogen in compounds **3b**, **4b**, and **5b** would influence the gel properties.

The synthesis commenced with conversion of pyridine-3,5-dicarboxylic acid **1** (**Figure 2**) to the corresponding acid chloride followed by condensation with the acrylate units **2**³¹ according to a modified procedure by van Koten³², and gave the pyridines **3a–5a** in 45%–63% yield. Subsequent N-methylation³³ provided the N-methylpyridinium salts **3b–5b** in 88%–90% yield. The obtained cross-linkers were used for the thiol-Michael reaction with HA-SH in aqueous media to give the corresponding hydrogels³⁴.

The gel formation of these HA-hydrogels was followed by measurements of the elasticity revealing very different degeneration behaviors: HA-hydrogels cross-linked with **3a** and **3b** form and degrade within 1 hour, while gels with **4a** degrade within a few hours and gels cross-linked with **4b** only form very weak gels (**Fig. S2**). In contrast, stable gels are formed with **5a** and **5b**. The E-moduli of these hydrogels with 1.0 cross-linker equiv. (defined as the number of acrylates divided by the number of thiols in the reaction) remained unchanged even after one week of incubation at 37°C in PBS

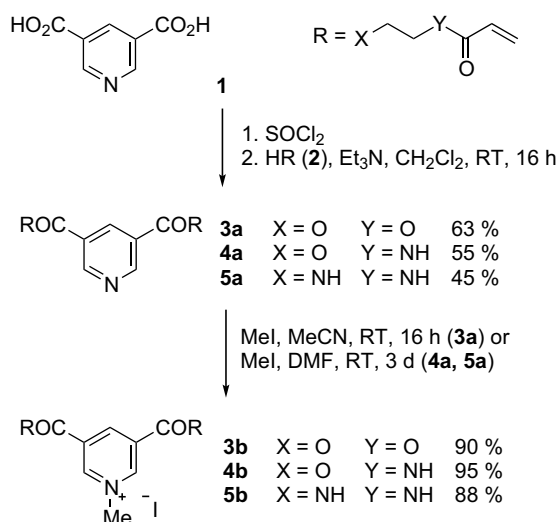


Figure 2 | Synthesis of the cross-linkers.

(**Table S1**), showing that the linkages are necessary for long-term stable gels.

Therefore, **5a** and **5b** were employed for subsequent characterization. Ellman's assay^{35,36} was used to quantify the efficiency of the cross-linking reaction between the acrylates in the linkers **5a** and **5b** and the thiols in HA-SH. The remaining free thiols were analyzed after 3 h of gelation in a range of 0 to 1.8 cross-linker equiv., (**Fig. 3**). Below 0.8 equiv. the reaction efficiencies are close to 100%, indicating the formation of cross-links to both arms of the linker. Higher cross-linker equiv. lead to slightly lower efficiencies, presumably due to steric hindrance. Furthermore, the reaction efficiency is not affected by the charge of the cross-linker as the data for both hydrogels show similar conversions.

The swelling ratios of HA-SH-**5a** hydrogels are generally lower than these of the corresponding HA-SH-**5b** hydrogels (**Fig. 4**). The lowest swelling ratio can be observed at about 0.8 equiv. increasing for both lower and higher amounts of cross-linker equiv. (**Fig. 4**).

The compression behavior of HA-SH-**5a** and HA-SH-**5b** hydrogels with 1.0 cross-linker equiv. was characterized in uniaxial compression tests (**Fig. 5**). The stress-strain data was recorded in the deformation range $0.55 < \lambda < 1$, where λ is the deformation ratio ($\lambda = L/L_0$, L and L_0 are the lengths of the deformed and undeformed samples). Measuring the nominal stress σ_n (related to the undeformed cross-section of the gel), these tests showed that the hydrogels withstand repetitive compression (5 cycles) up to $\lambda \approx 0.55$ with no damage or alterations (**Fig. 6**). Additionally both type of gels were found to show strain-stiffening behavior which is very accurately described by the form

$$\sigma_n = \frac{E}{3} \left(\lambda - \frac{1}{\lambda^2} \right) \exp \left(\frac{J_1}{m} \right); \quad J_1 = \lambda^2 + \frac{2}{\lambda} - 3 \quad (1)$$

where E represents the zero strain E-modulus and J_m a strain invariant at which strain hardening becomes dominant, thereby accounting for a finite extensibility of the polymeric chains. Equation (1) derives from a strain energy density³⁷, which was found to describe the elastic response of many biopolymer networks such as actin, collagen and vimentin^{38,39}.

From the fits for the HA-SH-**5a/b** gels with 1.0 cross-linker equiv. (**Fig. 5**) we found $J_m = 1.96$ and $J_m = 2.10$ respectively. Taking the obtained values of J_m and converting them to the maximum uniaxial extension ratio, λ_{max} , yields 1.99 (1.96, 2.01) and 2.03 (1.83, 2.20), indicating that the polymeric chains in the network can be extended to about twice their original length before the chains are strongly stiffening. Further, J_m can be converted to a maximum compression

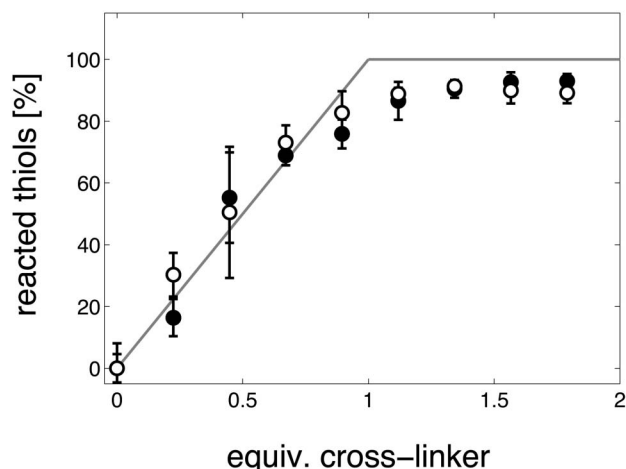


Figure 3 | Efficiency of cross-linking reaction between the cross-linkers **5a** (filled) and **5b** (empty) with HA-SH from 0 to 1.8 cross-linker equiv. as determined by an Ellman's assay. The solid line represents the ideal reaction efficiency.

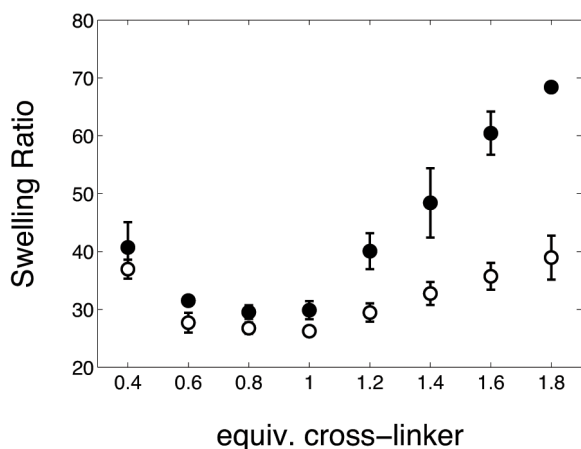


Figure 4 | Swelling ratio of HA-SH-5a (filled) and HA-SH-5b (empty) hydrogels. The hydrogels formed with the charged cross-linker **5b** show lower swelling ratios than the hydrogels formed with the neutral cross-linker **5a**. All experiments were performed in triplicates. Error bars represent SEM.

ratio $\lambda_{max,c}$ which yields 0.42 (0.41, 0.43) and 0.41 (0.36, 0.47). The fact that the values of λ_{max} are similar for both linkers indicates that the deformation of the hydrogels is mainly due to rearrangements of the polymeric backbones but not significantly influenced by the cross-linkers' charge. The change in the zero strain E-moduli and the value J_m over the five repeated compression cycles was lower than 10% for both type of linkers.

The long linear elastic regime of up to 10% compression (Fig. 5) enabled us to compare the zero strain E-moduli determined for different cross-linker equiv. values (Fig. 7). Gels formed with cross-linker equiv. between 0.8 and 1.0 show the highest elastic moduli. At 1.0 cross-linker equiv. $E = 7.1 \pm 1.2$ kPa for HA-SH-5a and $E = 4.2 \pm 0.5$ kPa for HA-SH-5b. Hydrogels formed with both higher and lower cross-linker equiv. resulted in softer gels with lower E-moduli; the increase of the elastic moduli up to 0.8 equiv. correlates with the increasing number of thiols reacting with the cross-linker up to this point. In the regime of up to 1.0 cross-linker equiv., hydrogels with the positively charged cross-linker **5b** show lower E-moduli than the hydrogels with the neutral cross-linker **5a**. At higher cross-linker equivalents, this trend is reversed (Fig. 7). Above a critical ratio corresponding to 1.6 equiv. for **5a** and 1.8 for **5b** no form-stable cylindrical gels could be created.

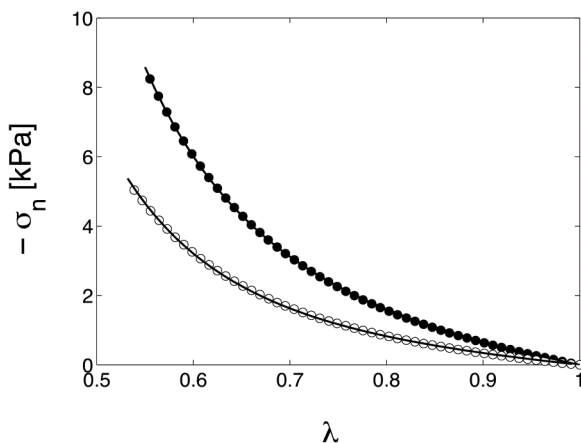


Figure 5 | Stress-strain curves for HA-SH-5a (filled) and HA-SH-5b (empty) hydrogels with 1.0 cross-linker equiv. σ_n represents the nominal stress, λ the deformation ratio. Solid black lines represent fitting curves based on equation (1), ($R^2 > 0.99$ for both fittings).

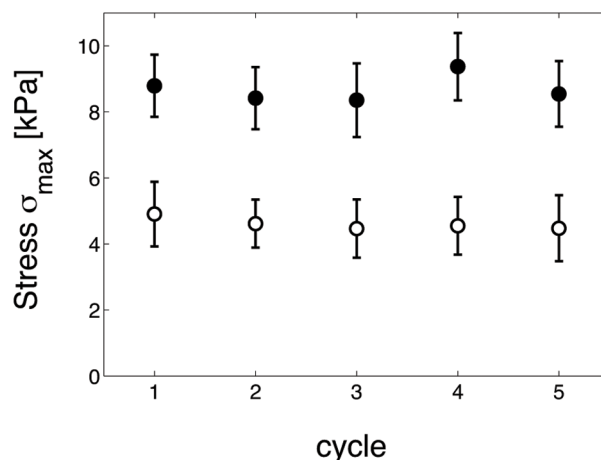


Figure 6 | For both gel types HA-SH-5a (filled) and HA-SH-5b (empty) the maximum stress σ_{max} at $\lambda = 0.55$ has been evaluated for the subsequent compression cycles which is showing that the gels are not damaged after 5 strong deformations. All experiments were performed in triplicates. Error bars represent SEM.

An initial in vitro cytotoxicity test was performed with primary fibroblasts, based on DIN ISO 10993-5 (Fig. S4). The cells maintain ~80% viability, compared to controls, after incubation with extracts of HA-SH-5a and HA-SH-5b hydrogels cross-linked with 1 and 1.5 cross-linker equiv. HA-SH-5a and HA-SH-5b were not found to release any toxic compounds in these tests.

Discussion

For implant materials, stability in aqueous medium at 37°C is important. We have found that HA-SH-5a/b hydrogels, where an amide containing linker was used, were stable when stored in PBS buffer at 37°C and did not decompose due to bond hydrolysis of the cross-linker. Soft biological tissues exhibit mechanical properties that are crucial to their functionality and are difficult to mimic with synthetic materials. In our system, the cross-linking density was found to be the main determinant of the gel stiffness, which allows for tuning of the gel properties in a range important for the engineering of soft tissues. The stiffest gels were obtained at ca. 0.8 cross-linker equiv., and the E-moduli were similar to those of human skin⁴⁰. Moreover, many biological materials show strain-stiffening at larger

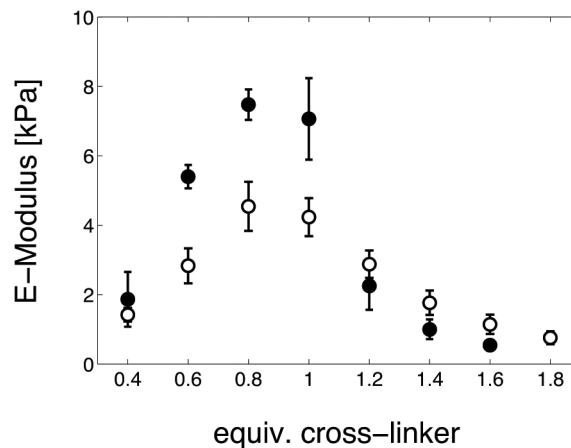


Figure 7 | E-moduli of HA-SH-5a (filled) and HA-SH-5b (empty) hydrogels measured by uniaxial compression testing between parallel plates. All experiments were performed in triplicates. Error bars represent SEM.



deformation, thereby preventing tissue damage. Such strain stiffening behavior was also observed for our HA-SH-5a/b hydrogels.

The Ellman's assay shows that the cross-linking within the HA-SH hydrogels is maximized at 0.8 equiv. Thus, up to 0.8 equiv. both acrylate arms of the cross-linker will react with the hyaluronan backbone, and at higher equivalents, an increasing number of cross-linkers are more likely to attach with only one arm to the hyaluronan backbone. Accordingly, hydrogels at 0.8 equiv. should exhibit the highest cross-link density. Hence, this is where the swelling ratio is lowest and the E-moduli is highest.

After the connectivity, the charge on the cross-linker is the second most important determinant of the hydrogel gel properties. Hyaluronan is overall a negatively charged biopolymer due to the carboxylic acid group on every second sugar unit, of which about half were modified to make HA-SH. Thus, with the neutral cross-linker 5a, the net charge on the hydrogel network is always negative. On the other hand, with the positively charged cross-linker 5b, the overall negative charge on the hydrogel network is reduced the more cross-linker that is added; the negative charge is only half as much as in the beginning when 1 equiv. of the cross-linker is added and is reduced even further at higher equivalents. The altered charge interactions in the hydrogel network influence the mechanical properties, especially the swelling ratio. At 0.4 cross-linker equiv. both hydrogels have similar mechanical properties since the negatively charged HA-SH dominates. At the higher equiv. the effect of the charge on the cross-linker becomes more pronounced and larger differences between HA-SH-5a and HA-SH-5b are observed.

In summary, we designed short, rigid cross-linkers for elastic hydrogels for tissue engineering, inspired by elastin and its natural cross-linker desmosine. The elastic similarity of our hyaluronan hydrogels HA-SH-5a,b to biological networks^{38,39} makes these gels a good candidate for biomedical applications. Furthermore, the possibility to vary the charge density without changing the network connectivity opens up new avenues to analyze charge-dependent cell behavior.

Methods

Cross-linker synthesis. Experimental procedures and characterizations of all synthesized products can be found in the supplemental information.

Hydrogel preparation. The thiolated hyaluronan (HA-SH) was synthesized as described in the literature⁴¹ with high molecular weight hyaluronan (Sigma-Aldrich) leading to HA-SH molecules with an average of 450 kDa. The number of thiol groups in HA-SH was quantified using the Ellman's assay^{35,36}. HA-SH was dissolved in PBS (Gibco) at 40 mg/ml and the pH was adjusted to 9.0. The cross-linkers were dissolved in a 50/50 (v/v) mixture PBS/ethanol at appropriate concentrations. All solutions used were degassed by sonication for 15 min to avoid oxidation reactions such as the formation of disulfide bonds.

For mechanical testing cylindrical hydrogels were formed. 70 μ l of HA-SH (49% thiolation) solution was mixed with 30 μ l of cross-linker solution giving a final HA-SH concentration of 2.8% in the gel. The mixture of the precursor solutions was gently vortexed for 3 s to obtain a homogeneous mixture. Thereafter the solution was immediately filled in cylindrical wells ($r = 3$ mm, $h = 3$ mm), closed with a glass slide and the mixture was left to gel for 24 h at 37°C. The hydrogels were then swollen to equilibrium for 48 h in PBS.

For the cell adhesion and cytotoxicity tests hydrogels (degree of thiolation 40%) were prepared in disk-shaped teflon forms ($r = 11$ mm; $h = 1.5$ mm) using the same method of preparation.

Ellman's assay. 40 μ l of the gelation mixture was prepared in eppendorf tubes (2 ml) that were subsequently flooded with nitrogen to avoid disulfide formation. After polymerization for 3 h at 37°C gels had formed in all tubes containing cross-linker solution. To the gels 784 μ l DTNB solution (50 mM sodium acetate, 2 mM 5,5'-Dithio-bis(2-nitrobenzoic acid) in H₂O) and 784 μ l Tris (1 M Tris/pH 8.0) was added. Thereafter the hydrogels were crushed into small pieces and incubated while shaking at 200 rpm for 20 min. 100 μ l from the supernatant was taken for the measurement and the absorption at 412 nm was measured with a plate reader. The percentage of reacted thiols was calculated as the absorption of the samples with different cross-linker concentrations divided by the absorption of the HA-SH solution without cross-linker.

Mechanical characterization. The mechanical properties of the HA-SH hydrogels were measured after equilibrium swelling was achieved on a MTS Nano Bionix

Testing System using a parallel plate geometry in compression mode. The hydrogel cylinders were freely sliding between the plates and not fixed in radial direction. Barrel shape formation at the cylinder side wall was avoided by leaving a thin film of solvent on the hydrogel surfaces such that the gels could preserve their cylindrical shape during deformation. For the measurement of the E-moduli stress-strain curves were recorded at a frequency set to 0.002 Hz. The analysis of the E-modulus was performed in the linear regime between 0 and 5% compression using a linear fit (linear range goes up to ca. 10% strain, see Figure 2). In high compression mode each hydrogel was subjected to five subsequent strains of at least 45%. Here the frequency was set to 0.003 Hz to avoid drying-out of the hydrogels during the measurement. All measurements were carried out in triplicates.

Fitting analysis. The data from the high compression measurements were fitted with equation (1) setting E to the zero strain modulus and thereby treating J_m as a single fitting parameter. To obtain λ_{max} , J_1 is set equal to the obtained J_m which yields two results, one of which relates to extension and a second one, $\lambda_{max,c}$ which relates to compression. The maximum extension ratio λ_{max} can be understood as l_{max}/l_0 where l_{max} is the length of a fully extended polymer chain and l_0 is the end-to-end distance of the unstretched polymer chain.

Swelling ratio. The swelling ratio of the hydrogels was taken as the wet weight of the hydrogels after swelling to equilibrium in PBS divided by the dry weight of the hydrogels which was calculated from the polymer and cross-linker concentration used and the volume of the cylindrical wells.

Long term stability. For the measurement of the long term stability the HA-SH (58% thiolation) hydrogels were stored in PBS at 37°C for up to a week and the mechanical properties were measured as described above.

- van Vlierberghe, S., Dubruel, P. & Schacht, E. Biopolymer-Based Hydrogels As Scaffolds for Tissue Engineering Applications: A Review. *Biomacromolecules* **12**, 1387–1408 (2011).
- Burdick, J. A. & Prestwich, G. D. Hyaluronic acid hydrogels for biomedical applications. *Adv. Mater.* **23**, H41–56 (2011).
- Truong, W. T. *et al.* Self-Assembled Gels for Biomedical Applications. *Chem. Asian J.* **6**, 30–42 (2011).
- Nichol, J. W. & Khademhosseini, A. Modular tissue engineering: engineering biological tissues from the bottom up. *Soft Matter* **5**, 1312 (2009).
- Yu, L. & Ding, J. Injectable hydrogels as unique biomedical materials. *Chem. Soc. Rev.* **37**, 1473 (2008).
- Peppas, N. A., Hilt, J. Z., Khademhosseini, A. & Langer, R. Hydrogels in Biology and Medicine: From Molecular Principles to Bionanotechnology. *Adv. Mater.* **18**, 1345–1360 (2006).
- Lee, K. Y. & Mooney, D. J. Hydrogels for Tissue Engineering. *Chem. Rev.* **101**, 1869–1880 (2001).
- Sisson, A. L. & Haag, R. Polyglycerol nanogels: highly functional scaffolds for biomedical applications. *Soft Matter* **6**, 4968 (2010).
- Cruise, G. M., Scharp, D. S. & Hubbell, J. A. Characterization of permeability and network structure of interfacially photopolymerized poly(ethylene glycol) diacrylate hydrogels. *Biomaterials* **19**, 1287–1294 (1998).
- Zhang, H. *et al.* Controllable properties and microstructure of hydrogels based on crosslinked poly(ethylene glycol) diacrylates with different molecular weights. *J. Appl. Polym. Sci.* **121**, 531–540 (2011).
- Prestwich, G. & Kuo, J.-W. Chemically-Modified HA for Therapy and Regenerative Medicine. *Curr. Pharm. Biotechnol.* **9**, 242–245 (2008).
- DeAngelis, P. L. Hyaluronan synthases: fascinating glycosyltransferases from vertebrates, bacterial pathogens, and algal viruses. *Cell. Mol. Life Sci.* **56**, 670–682 (1999).
- Laurent, T. C., Laurent, U. B. G. & Fraser, J. R. E. The structure and function of hyaluronan: An overview. *Immunol. Cell Biol.* **74**, A1 (1996).
- Bashur, C. A., Venkataraman, L. & Ramamurthi, A. Tissue Engineering and Regenerative Strategies to Replicate Biocomplexity of Vascular Elastic Matrix Assembly. *Tissue Eng. Pt. B* **18**, 203–217 (2012).
- Seliktar, D. Designing Cell-Compatible Hydrogels for Biomedical Applications. *Science* **336**, 1124–1128 (2012).
- Shu, X. Z., Liu, Y., Palumbo, F. S., Luo, Y. & Prestwich, G. D. In situ crosslinkable hyaluronan hydrogels for tissue engineering. *Biomaterials* **25**, 1339–1348 (2004).
- Shu, X. Z., Ahmad, S., Liu, Y. & Prestwich, G. D. Synthesis and evaluation of injectable, in situ crosslinkable synthetic extracellular matrices for tissue engineering. *J. Biomed. Mater. Res.* **79**, 902–912 (2006).
- Schneider, G. B. *et al.* The effect of hydrogel charge density on cell attachment. *Biomaterials* **25**, 3023–3028 (2004).
- Fischer, D., Li, Y., Ahlemeyer, B., Kriegelstein, J. & Kissel, T. In vitro cytotoxicity testing of polycations: influence of polymer structure on cell viability and hemolysis. *Biomaterials* **24**, 1121–1131 (2003).
- Chen, Y. M. *et al.* Tuning of cell proliferation on tough gels by critical charge effect. *J. Biomed. Mater. Res.* **88**, 74–83 (2009).
- Chen, Y. M., Ogawa, R., Kakugo, A., Osada, Y. & Gong, J. P. Dynamic cell behavior on synthetic hydrogels with different charge densities. *Soft Matter* **5**, 1804 (2009).



22. Kaga, N. *et al.* Quantification of elastin cross-linking amino acids, desmosine and isodesmosine, in hydrolysates of rat lung by ion-pair liquid chromatography–mass spectrometry. *Anal. Biochem.* **318**, 25–29 (2003).
23. Wang, Q. *et al.* High-water-content mouldable hydrogels by mixing clay and a dendritic molecular binder. *Nature* **463**, 339–343 (2010).
24. Umeda, H., Aikawa, M. & Libby, P. Liberation of desmosine and isodesmosine as amino acids from insoluble elastin by elastolytic proteases. *Biochem. Biophys. Res. Commun.* **411**, 281–286 (2011).
25. Akagawa, M. & Suyama, K. Mechanism of formation of elastin crosslinks. *Connect. Tissue Res.* **41**, 131–141 (2000).
26. Eyre, D. R., Paz, M. A. & Gallop, P. M. Cross-linking in collagen and elastin. *Annu. Rev. Biochem.* **53**, 717–748 (1984).
27. Skinner, S. Rapid method for the purification of the elastin cross-links, desmosine and isodesmosine. *J. Chromatogr. B* **229**, 200–204 (1982).
28. Anwar, R. A. & Oda, G. The biosynthesis of desmosine and isodesmosine. II. Incorporation of specifically labeled lysine into desmosine and isodesmosine. *Biochim. Biophys. Acta* **133**, 151–156 (1967).
29. Thomas, J., Elsdon, D. F. & Partridge, S. M. Degradation Products from Elastin: Partial Structure of Two Major Degradation Products from the Cross-linkages in Elastin. *Nature* **200**, 651–652 (1963).
30. Katritzky, A., Ramsden, C., Joule, J. & Zhdankin, V. *Handbook Of Heterocyclic Chemistry*. 3rd ed. (Elsevier, Oxford, 2010).
31. Hobson, L. J. & Feast, W. Poly(amidoamine) hyperbranched systems: synthesis, structure and characterization. *Polymer* **40**, 1279–1297 (1999).
32. Chuchuryukin, A. *et al.* General Approach for Template-Directed Synthesis of Macroheterocycles by Ring-Closing Metathesis (RCM). *Adv. Synth. Catal.* **347**, 447–462 (2005).
33. Meyer, H. Über Esterbildung und Betaine. *Monatsh. Chem.* **24**, 195–208 (1903).
34. Boehm, H. *et al.* Novel Cross-linkers for Hyaluronan Hydrogels, Hydrogels Including these Cross-linkers and Applications thereof, PCT/EP2012/004014.
35. Ellman, G. L. A colorimetric method for determining low concentrations of mercaptans. *Arch. Biochem. Biophys.* **74**, 443–450 (1958).
36. Thannhauser, T. W., Konishi, Y. & Scheraga, H. A. Analysis for disulfide bonds in peptides and proteins. *Methods in Enzymology* **143**, (Sulfur and Sulfur Amino Acids) 115–119 (1987).
37. Seitz, M. E. *et al.* Fracture and large strain behavior of self-assembled triblock copolymer gels. *Soft Matter* **5**, 447 (2009).
38. Storm, C., Pastore, J. J., MacKintosh, F. C., Lubensky, T. C. & Janmey, P. A. Nonlinear elasticity in biological gels. *Nature* **435**, 191–194 (2005).
39. Erk, K. A., Henderson, K. J. & Shull, K. R. Strain Stiffening in Synthetic and Biopolymer Networks. *Biomacromolecules* **11**, 1358–1363 (2010).
40. Zheng, Y. & Mak, A. Extraction of effective Young's modulus of skin and subcutaneous tissues from manual indentation data. *19th Annual International Conference of the IEEE Engineering in Medicine and Biology Society*. 2246–2249 (1997).
41. Shu, X. Z., Liu, Y., Luo, Y., Roberts, M. C. & Prestwich, G. D. Disulfide Cross-Linked Hyaluronan Hydrogels. *Biomacromolecules* **3**, 1304–1311 (2002).

Acknowledgements

This work was supported by the Ministry of Science, Research, and the Arts of Baden-Wuerttemberg (Az: 720.830- 5-10a), the Fonds der Chemischen Industrie and the Max Planck Society. S.V.W. thanks the Alexander von Humboldt Foundation for a fellowship. C.S. thanks the Peter und Traudl-Engelhorn-Stiftung for funding. We thank N. Klechowicz for help with the cell experiments. J.P. Spatz is the Weston Visiting Professor at the Weizmann Institute of Science. We thank C. Cobley for proofreading.

Author contributions

S.L. and H.B. wrote the main manuscript text. M.M. and A.S. adapted the chemical structures of the crosslinkers for stable hydrogels. M.M. carried out the synthetic procedures and prepared the schemes 1–2 (and part of the supporting information). S.V.W. synthesized thiolated H.A. V.H. and I.N. carried out the hydrogel characterisation. V.H. prepared figures 1–5. T.H. performed the theoretical analysis. C.K. performed the cell viability experiments (supporting information). C.S., G.E.M.T., J.P.S., M.B., P.J.K. and S.T. supported the work with their expert opinions and reviewed the manuscript.

Additional information

Supplementary information accompanies this paper at <http://www.nature.com/scientificreports>

Competing financial interests: The authors declare no competing financial interests.

How to cite this article: Hagel, V. *et al.* Desmosine-Inspired Cross-Linkers for Hyaluronan Hydrogels. *Sci. Rep.* **3**, 2043; DOI:10.1038/srep02043 (2013).



This work is licensed under a Creative Commons Attribution-NonCommercial-NoDerivs 3.0 Unported license. To view a copy of this license, visit <http://creativecommons.org/licenses/by-nc-nd/3.0>